

Scientific Spokesman:

John Elias  
Fermilab  
840-4135

INCLUSIVE POWER LAW DISTRIBUTIONS FOR NON-LEADING  
PARTICLES PRODUCED IN HADRON COLLISIONS

A. E. Brenner, D. C. Carey, J. E. Elias, P. H. Garbincius  
and V. A. Polychronakos  
Fermi National Accelerator Laboratory, Batavia, Illinois 60510

and

D. Cutts, R. Dulude, R. E. Lanou, and J. T. Massimo  
Brown University, Providence, Rhode Island 02912

and

M. T. Chiaradia, C. DeMarzo, C. Favuzzi, G. Germinario,  
L. Guerriero, P. LaVopa, G. Maggi, F. Posa, G. Selvaggi,  
P. Spinelli and F. Waldner  
Istituto di Fisica and INFN, Bari, Italy

January 27, 1978

*23pp.*

INCLUSIVE POWER LAW DISTRIBUTIONS FOR NON-LEADING  
PARTICLES PRODUCED IN HADRON COLLISIONS

A. Brenner, D. Carey, J. Elias, P. Garbincius, V. Polychronakos (Fermilab); D. Cutts, R. Dulude, R. Lanou, J. Massimo (Brown University); M. Chiaradia, C. DeMarzo, C. Favuzzi, G. Germinario, L. Guerriero, P. LaVopa, G. Maggi, F. Posa, G. Selvaggi, P. Spinelli, F. Waldner (Istituto di Fisica and INFN)

A study of single particle inclusive spectra using the Single Arm Spectrometer (SAS) in the M6E beam line is proposed. The principal objective is a determination of the power law behavior,  $(1-x)^n$ , of non-leading reactions in the beam fragmentation region. This experiment which extends the measurements made earlier in E-118A will span a kinematic range of  $.3 < x < .88$  mostly at  $p_T=0.3$  and  $0.5$  at an incident momentum of  $\bar{100}$  GeV/c. Particular emphasis will be placed on reactions initiated by kaons and  $\bar{p}$ 's. Most of the minority channels will be measured to the 10-20% level.

Recent work, both experimental and theoretical, has indicated that hadron-hadron inclusive reactions at small as well as large  $p_T$  provide considerable insight into the understanding of the internal structure of the hadrons. Kaon initiated reactions will provide information on the valence  $s$  and  $\bar{s}$  distributions in the kaon, and similarly, the inclusive kaon spectra would probe  $s$  and  $\bar{s}$  distributions in the hadron sea.

This experiment uses the apparatus of E-118A, with the deletion of the target area multiplicity detector. This allows for an incident flux of 5-10 times that which was possible in the earlier experiment. The  $\pi^0$  detector built for E-451 (also an SAS experiment) will be the only added piece of equipment.

The  $\pi^0$  detector will be used to implement a second independent trigger to simultaneously study inclusive  $\pi^0$  spectra in the range  $0 < x_R < 0.8$  and with  $p_T$  up to  $\sim 4.0$ . This measurement will improve existing data by about an order of magnitude in sensitivity and will explore a new kinematic region.

With a flux of  $10^7$  particles onto the hydrogen target per accelerator pulse, the measurements will require 500 hours of average quality beam time. An additional 100 hours will be required for start-up and spectrometer tuning.

January, 1978

internal structure of hadrons. Recently, experimental evidence has prompted attempts to extend the quark-parton ideas to include low  $p_T$  phenomena. In particular, a relationship has been observed between the longitudinal spectra of pions produced in proton-proton interactions at high energies and the quark structure functions as measured in lepton-proton interactions. Therefore, low  $p_T$  phenomena are proving to be important in understanding the internal structure of hadrons, especially the dynamics of multiparticle production from elementary constituent interactions.

We propose to extend our investigation of single particle inclusive spectra in the projectile fragmentation region by an intensive concentration on those rarer channels which could not be adequately covered in our recently completed survey experiment, E118A. In particular, we wish to concentrate on kaon and  $\bar{p}$  driven reactions, plus a few other rare processes. A modest alteration in our apparatus will allow an order of magnitude greater sensitivity to these reactions. Our E118A results have allowed rough estimates of the rates of these reactions, and have guided our proposal for further investigation. Combined with our results from E118A, these new data will provide measurements of inclusive cross sections for a wide variety of incident and produced particle types. This will be essential in unraveling the influence of constituent type on the dynamics of multiparticle production. Thus, we can possibly establish the link between the short-range high transverse momentum

phenomena and the relatively long-range low  $p_T$  interactions.

## II. PHYSICS BACKGROUND

The preliminary analysis of experiment E118A and other FNAL and ISR experiments support the idea that there exists an underlying connection between low  $p_T$  phenomena and quark-parton ideas. The ISR data first showed that the inclusive pion spectra in pp interactions exhibit a power law behaviour similar to the observed  $\nu W_2(x)$  at SLAC, i.e.,  $d\sigma/dx(pp \rightarrow \pi^+X) \sim (1-x)^3$ . This led Ochs<sup>(3)</sup> to speculate that these pions are fragments of the quarks in the proton. Brodsky and Gunion<sup>(4)</sup> then cite Ochs<sup>(3)</sup> in predicting that at large  $x$ <sup>(4)</sup>

$$R(\pi^+/\pi^-) = \frac{d\sigma/dx(pp \rightarrow \pi^+X)}{d\sigma/dx(pp \rightarrow \pi^-X)} = \frac{G_u/p(x)}{G_d/p(x)}$$

where  $G_{u/p}(x)$  and  $G_{d/p}(x)$  are the u and d quark distributions in a proton respectively. It then follows that

$$\frac{\nu W_2^{en}}{\nu W_2^{ep}} = \frac{4+R}{4R+1}$$

This relation is well satisfied over the range  $0 < x < 1$  as shown in Figure 1, which is reproduced from Reference 3. Furthermore, the ratio  $R$  appears to be approaching 5 at  $x \rightarrow 1$  or equivalently  $\nu W_2^{en}/\nu W_2^{ep} \rightarrow 3/7$  a value predicted by Farrer and Jackson<sup>(5)</sup> in a quark-vector gluon model if the helicities of the proton and the leading quark are the same for  $x \rightarrow 1$ . In addition,  $R$  appears to be independent of  $p_T$ . In Figure 2,  $R$ , as calculated from our E118A data, is plotted against  $x$  along with the values from

Antreasyan et. al.,<sup>(6)</sup> from a high  $p_T$  experiment plotted against  $x_{\perp}$ . It appears that R has the same behaviour as  $x \rightarrow 1$  in the beam direction and as  $x_{\perp} \rightarrow 1$  at  $90^\circ$ . The same appears to be true with the  $K^+/K^-$  ratio as shown in Figure 3.\*

Yet another aspect of the power law behaviour of the inclusive spectra seems to favour the quark-parton model. In Figures 4 and 5 the x-distributions are plotted for various particle species in  $\pi^+$  and p induced reactions respectively at  $p_T = 0.3$  GeV/c and incident momentum of 100 GeV/c. The solid lines in these figures represent fits of the data to the form  $A(1-x)^{n_h}$ . The values of the exponent  $n_h$  are tabulated in Table I for the various hadrons. In the same table the exponents from fits to the data at  $p_T = 0.5$  and  $0.75$  GeV/c are shown. They appear to be nearly independent of  $p_T$  at least in the  $p_T$  region between 0.3 and 0.8 GeV/c. This constant power law behaviour is characteristic of most constituent models<sup>(7,8)</sup>, in contrast to predictions from multi-Regge expansions in which the distributions behave as  $d\sigma/dxdt \sim \beta(t)(1-x)^{1-2\alpha(t)}$  where  $\alpha(t)$  is the leading trajectory and the power should approach zero at small  $t \sim p_T^2$ .

As the quark-parton models become more quantitative one expects that the longitudinal inclusive spectra will be of great importance in understanding the constituent picture of hadrons. In particular, we will look at mesons, which cannot be studied in lepton-induced reactions. The "unfavoured" reactions

---

\* Similar behaviour was observed by J. R. Johnson et. al.<sup>(10)</sup> who plot their data as a function of  $x_R = E^*/E_{\max}$ .

e.g.,  $\pi^+p \rightarrow K^-X$ ,  $pp \rightarrow K^-X$  which we intend to emphasize in this experiment should be particularly useful since they are free from leading particle and other effects which make the interpretation of "favoured" processes more difficult. Kaon spectra for example, probe the  $s$  and  $\bar{s}$  distributions in the hadron sea, whereas kaon induced reactions provide information on the valence  $s$  and  $\bar{s}$  distributions in these mesons. An attempt to this direction has already been made by Duke and Taylor<sup>(9)</sup> who used data from a FNAL experiment<sup>(10)</sup> to determine the sea distributions in the proton with some interesting results as to the fraction of momentum carried by the sea quarks.

### III. THE PROPOSED EXPERIMENT

We propose to pursue further the exploration of single particle inclusive reactions started with E118A using the Single Arm Spectrometer (SAS) and the M6E beam line. The spectrometer has been successfully operating for several years and has been described elsewhere<sup>(11)</sup>. Briefly we can measure and identify hadrons produced with momentum between  $P_{\max}$  and 20 GeV/c and at angles between 3 and 19 mr in the laboratory system. The corresponding Feynman- $x$  range extends from  $x = 0.2$  to  $x = 0.95$  for 100 GeV/c incident momentum. The range for  $p_T$  is from  $p_T \approx 0$  to  $p_T \approx 1.2$  GeV/c.

This experiment differs from E118A in that we do not plan to use the associated charged multiplicity detector used in E118A. This will enable us to increase the incident flux by a factor of 5 to 10 improving the statistical accuracy for the "minority"

or "unfavoured" channels. Prescaling of the dominant incident particles will allow further emphasis of the minority channels. In addition, the target empty background rate will be reduced to about 4% of the target full rate.

Another major difference is the use in this experiment of the  $\pi^0$  detector being installed for experiment E451. This detector will be used as a second independent trigger to study inclusive  $\pi^0$  spectra over the wide kinematic range shown in Figure 6. The detector is centered at 90 mrad in the LAB (65 degrees in the CM), allowing simultaneous coverage of both the central  $x \approx 0$  region and the fragmentation region out to the kinematic limit at  $p_T = 3.0$  GeV/c. The  $\pi^0$  detector subtends 15 mster in the Laboratory and will determine the  $p_T$  of the  $\pi^0$  to about 10% by measuring the shower position and energy. This will allow, for the first time, an extensive coverage in  $x$  and  $p_T$  for inclusive  $\pi^0$  production by both proton and meson beams.

Two other groups working at Fermilab have studied  $\pi^0$  production. E63 studied radial scaling<sup>(12)</sup> in pp interactions and E268 compared the production of  $\pi^0$  by proton and pion beams<sup>(13)</sup> at essentially 90° in the center of mass. We propose to study the ratio

$$E \frac{d^3\sigma}{dp^3} (\pi^+ p \rightarrow \pi^0 X) \Bigg/ E \frac{d^3\sigma}{dp^3} (pp \rightarrow \pi^0 X)$$

as a function of both  $x$  and  $p_T$ , extending coverage in the radial  $x$  variable to  $x_R \approx 0.8$  and a major improvement in statistics at lower  $x_R$ .

Our preliminary plans are to restrict ourselves to an incident momentum of 100 GeV/c only and to accumulate data at  $p_T = 0.3$ , and  $p_T = 0.5$  GeV/c for all 4 combinations of charge sign in the beam and the spectrometer. The  $x$ -range to be covered will extend from  $x = 0.3$  to  $x = 0.88$ . In addition, data will be taken at  $p_T = 0.75$  for one  $x$ -value only,  $x = 0.3$ , to complement existing data from E118A and provide a  $p_T$  dependence of the cross sections from  $p_T \sim .15$  GeV/c to  $p_T = .75$  GeV/c.

#### IV. RATES AND RUNNING TIME

The expected counting rates per one hour running time for all possible channels are shown in Table II. All the rates were calculated at  $x = 0.3$  and  $p_T = 0.3$  GeV/c and are based on the following conditions.

- 1) The cross sections were taken from the preliminary E118A results. To calculate rates at kinematic points where no data were available the measured  $p_T$  and  $x$  dependence for the appropriate channels were used to extrapolate the measured cross sections to these points.
- 2) The spectrometer tune used is the same as in E118A. It provides an effective phase space acceptance of 32  $\mu$ ster%.
- 3) The same 20" liquid hydrogen target as in E118A was used.

- 4) An incident flux of  $10^7$  particles per accelerator pulse was used with the particle composition shown in Table III.

Experiment E99 recently ran at the facility at comparable rates experienced no problems with the beam tagging system other than a slight increase of double buckets. Finally, we estimated a pulse repetition rate of 5 pulses/minute.

The total running time required to accumulate enough events for a 10 to 20% statistical accuracy for most minority channels, at  $p_T = 0.3$  and  $0.5$  GeV/c, is estimated to be approximately 500 hours. It has been our experience that an additional 50 to 100 hours is required for start-up and spectrometer tune. In Table IV are shown the time estimates for 10% statistics for the indicated minority channel as well as estimated yields for certain other minority channels for positive beam. Table V shows the same for negative beam. Finally in Table VII are shown the yields for selected channels for a 12 hour run at  $p_T = 0.75$  GeV/c.

The same luminosity considerations were used to calculate the expected rates in the  $\pi^0$  detector. We again emphasize that only one setting is required to cover the kinematic range outlined in Figure 1. The proton induced rate was based on an extrapolation of the radial scaling parametrization.<sup>(12)</sup> The pion/proton beam ratios at all  $x$  were assumed to be those measured at  $90^\circ$  in the center of mass.<sup>(13)</sup> Table VI lists the data rate per hour in a bin  $\Delta p_T = 1.0$  GeV/c, and  $\Delta x = 0.10$  centered for  $p_T = 3.0$  GeV/c for various  $x$  values. This shows that we can obtain a 10%

measurement of the cross sections at  $p_T = 3.0$  GeV/c out to

$x = 0.45$  for  $pp \rightarrow \pi^0 X$

$x = 0.55$  for  $\pi^+ p \rightarrow \pi^0 X$

$x = 0.62$  for  $\pi^- p \rightarrow \pi^0 X$

## REFERENCES

1. R. P. Feynman, Photon-Hadron Interactions (W. A. Benjamin, New York, 1972); Phys. Rev. Letters 23, 1415(1969).
2. For a review see J. I. Friedman and H. W. Kendall, Rev. Nucl. Sci. 22, 203(1972).
3. W. Ochs, Nucl. Phys. B118, 397(1977).
4. S. J. Brodsky and J. F. Gunion, SLAC-PUB-1820(1976).
5. G. R. Farrar and D. R. Jackson, Phys. Rev. Letters 35,1416(1975).
6. D. Antreasyan et al., Phys. Rev. Letters 38, 112(1977).
7. R. Blankenbecler and S. Brodsky, Phys. Rev. D10, 2973(1974).
8. H. Goldberg, Nucl. Phys. B44, 149(1972).
9. D. W. Duke and F. E. Taylor, FERMILAB-Pub-77/95(1977).
10. J. R. Johnson et al., FERMILAB-Pub-77/98(1977), and FERMILAB-Pub-77/99(1977).
11. J. Butler, Ph.D. Thesis, unpublished, MIT(1975); D. S. Ayres et al., Phys. Rev. D15, 3105(1977).
12. D. C. Carey et al., Phys. Rev. D14,1196(1976).
13. G. Donaldson et al., Phys. Rev. Letters 36,1110(1976).

## TABLE CAPTIONS

- TABLE I Exponents of the power law fits to the E118A data.
- TABLE II Event rate/hr for  $10^7$  incident particles/pulse and 5 pulses/min at  $x=0.3$ .
- TABLE III Composition of the M6E beam line for 400 GeV/c primary protons.
- TABLE IV Run plan and estimated yields for selected channels initiated by positive beam.
- TABLE V Run plan and estimated yields for selected channels initiated by negative beam.
- TABLE VI  $\pi^0$  event rate/hr for  $10^7$  incident particles/pulse and 5 pulses/min at 100 GeV/c incident momentum and at  $x=0.3$ .
- TABLE VII Estimated yields for selected channels for 6 hours running time at  $p_T=0.75$  GeV/c and  $x=0.3$ .

## FIGURE CAPTIONS

Fig. 1: Comparison of the neutron-proton ratio in deep inelastic scattering, and inclusive  $\pi^\pm$  production in pp interactions (Ref. 3 and references therein).

Fig. 2: Ratios of the invariant cross sections for  $\pi^+$ , and  $\pi^-$  production from experiment E118A, and from an experiment at  $90^\circ$  in the CM (Ref. 6).

Fig. 3: Ratios of the invariant cross sections for  $K^+$ , and  $K^-$  production from experiment E118A, and from an experiment at  $90^\circ$  in the CM (Ref. 6).

Fig. 4: Invariant cross sections for the production of  $\pi^+$  (x),  $\pi^-$  (•),  $K^+$  (▲),  $K^-$  (▼), p (■),  $\bar{p}$  (◆) in  $\pi^+p$  interactions as functions of Feynman-x at 100 GeV/c incident momentum, and at  $p_T=0.3$  GeV/c (from E118A).

Fig. 5: Invariant cross sections for the production of  $\pi^+$  (•),  $\pi^-$  (◆),  $K^+$  (▲),  $K^-$  (▼), p (+),  $\bar{p}$  (■) in pp interactions as functions of Feynman-x at 100 GeV/c incident momentum, and at  $p_T=0.3$  GeV/c (from E118A).

Fig. 6: Acceptance of the  $\pi^0$  detector positioned as described in the text, and at incident momentum of 100 GeV/c.

TABLE I  
 EXPONENTS OF THE POWER LAW FITS TO THE E118A DATA

		$\pi^+ p \rightarrow hX$			$pp \rightarrow hX$		
h	$P_T$	$n_h$	Average $n_h$	h	$P_T$	$n_h$	Average $n_h$
$K^+$	0.3	$0.56 \pm 0.11$		$K^+$	0.3	$2.89 \pm 0.12$	
	0.5	$0.68 \pm 0.07$	$0.73 \pm 0.05$		0.5	$2.93 \pm 0.09$	$2.94 \pm 0.06$
	0.75	$0.97 \pm 0.10$			0.75	$3.01 \pm 0.12$	
p	0.3	$1.53 \pm 0.13$		$K^+$	0.3	$1.60 \pm 0.22$	
	0.5	$1.30 \pm 0.09$	$1.39 \pm 0.06$		0.5	$2.01 \pm 0.12$	$1.95 \pm 0.09$
	0.75	$1.42 \pm 0.11$			0.75	$2.06 \pm 0.19$	
$\pi^-$	0.3	$1.10 \pm 0.10$		$\pi^-$	0.3	$3.66 \pm 0.14$	
	0.5	$1.99 \pm 0.18$	$1.47 \pm 0.07$		0.4	$4.20 \pm 0.12$	$3.92 \pm 0.08$
	0.75	$1.82 \pm 0.13$			0.5	$3.78 \pm 0.16$	
$K^-$	0.3	$1.83 \pm 0.14$		$K^-$	0.3	$4.45 \pm 0.28$	$4.42 \pm 0.24$
	0.5	$2.43 \pm 0.32$	$1.89 \pm 0.11$		0.5	$4.33 \pm 0.46$	
	0.75	$1.80 \pm 0.20$					
$\bar{p}$	0.3	$2.42 \pm 0.18$	$2.43 \pm 0.16$	$\bar{p}$	0.3	$6.06 \pm 0.47$	$6.65 \pm 0.13$
	0.5	$2.46 \pm 0.32$			0.5	$6.69 \pm 0.13$	

TABLE II  
EVENT RATE/HR FOR  $10^7$  INCIDENT PARTICLES/  
PULSE AND 5 PULSES/MIN  
 $x=0.3$

		100 GeV/c		$p_T=0.3$ GeV/c			
In	Out	$\pi^+$	$K^+$	p	$\pi^-$	$K^-$	$\bar{p}$
$\pi^+$		3491	371	299	1903	262	137
$K^+$		146	103	11	117	17	12
p		2012	181	1808	939	64	20
$\pi^-$		2697	334	356	5410	451	304
$K^-$		103	21	10	178	125	11
$\bar{p}$		106	31	11	180	7	123

		100 GeV/c		$p_T=0.5$ GeV/c			
In	Out	$\pi^+$	$K^+$	p	$\pi^-$	$K^-$	$\bar{p}$
$\pi^+$		1298	213	210	930	91	65
$K^+$		91	65	10	42	5	5
p		862	141	923	432	22	15
$\pi^-$		1519	147	182	2795	272	176
$K^-$		32	26	13	74	42	9
$\bar{p}$		62	15	5	65	4	77

TABLE III  
COMPOSITION OF THE M6E BEAM LINE  
FOR 400 GeV/c PRIMARY PROTONS

Secondary momentum	p	$\pi^+$	$K^+$	$\bar{p}$	$\pi^-$	$K^-$
100 GeV/c	0.380	0.570	0.039	0.034	0.920	0.047
150 GeV/c	0.630	0.330	0.032	0.022	0.940	0.049
175 GeV/c	0.720	0.230	0.030	0.015	0.950	0.044

TABLE IV  
 RUNPLAN AND ESTIMATED YIELDS FOR SELECTED CHANNELS INITIATED BY POSITIVE BEAM

$P_T = 0.3 \text{ GeV}/c$		$P_T = 0.5 \text{ GeV}/c$		
		1. +BEAM	+SAS	
x	(hrs)	(events)	(events)	
Time	$K^+ \rightarrow p$	$K^+ \rightarrow p^+ K^+$	$K^+ \rightarrow K^+ K^+$	
0.3	4.0	50	580	400
0.4	4.0	50	1100	960
0.5	4.0	50	1400	1140
0.6	5.0	50	2670	1400
0.7	5.0	50	580	1600
0.8	5.0	50	860	3750
0.88	5.0	35	430	5700

$P_T = 0.3 \text{ GeV}/c$		$P_T = 0.5 \text{ GeV}/c$		
		2. +BEAM	-SAS	
x	(hrs)	(events)	(events)	
Time	$K^+ \rightarrow \pi^-$	$\pi^- \rightarrow \bar{p}$	$K^+ \rightarrow K^- K^+$	
0.3	2.5	300	250	30
0.4	2.5	300	250	20
0.5	3.0	300	300	30
0.6	3.5	300	350	20
0.7	3.5	300	250	20
0.8	4.0	300	80	80
0.88	4.0	200	70	70

x	(hrs)	Time	$K^+ \rightarrow \pi^-$	$K^+ \rightarrow K^- K^+$	$K^+ \rightarrow \bar{p}$	$p \rightarrow K^-$	$p \rightarrow \bar{p}$	$p \rightarrow K^-$	$p \rightarrow \bar{p}$
		1.5	300	600	200	45			
		1.5	300	600	270	35			
		2.0	300	400	600	20			
		2.0	300	400	650	20			
		2.5	300	500	900	15			
		2.5	300	250	2400	3			
		3.0	300	300	3000				

x	(hrs)	Time	$K^+ \rightarrow \pi^-$	$K^+ \rightarrow K^- K^+$	$K^+ \rightarrow \bar{p}$	$p \rightarrow K^-$	$p \rightarrow \bar{p}$
0.3	2.5	100	14	30	55	37	
0.4	2.5	100	13	25	45	20	
0.5	2.5	100	12	25	40	9	
0.6	2.5	100	5	10	20		
0.7	3.0	100		4			
0.8	3.0	100					
0.88	3.0	100					

TABLE V

RUN PLAN AND ESTIMATED YIELDS FOR SELECTED CHANNELS INITIATED BY NEGATIVE BEAM

		1. -BEAM $\rightarrow$ -SAS				2. -BEAM $\rightarrow$ +SAS			
		$P_T = 0.3$ GeV/c		$P_T = 0.5$ GeV/c		$P_T = 0.3$ GeV/c		$P_T = 0.5$ GeV/c	
(hrs)	(events)	(hrs)	(events)	(hrs)	(events)	(hrs)	(events)	(hrs)	(events)
x Time	$\bar{p} \rightarrow \pi^-$ $\bar{p} \rightarrow K^-$ $K^- \rightarrow \pi^-$ $K^- \rightarrow K^-$ $K^- \rightarrow \bar{p}$	Time	$\bar{p} \rightarrow \pi^-$ $\bar{p} \rightarrow K^-$ $K^- \rightarrow \pi^-$ $K^- \rightarrow K^-$ $K^- \rightarrow \bar{p}$	Time	$\bar{p} \rightarrow \pi^-$ $\bar{p} \rightarrow K^-$ $K^- \rightarrow \pi^-$ $K^- \rightarrow K^-$ $K^- \rightarrow \bar{p}$	Time	$K^- \rightarrow \pi^+$ $K^- \rightarrow K^+$ $K^- \rightarrow p$ $\bar{p} \rightarrow \pi^+$ $\bar{p} \rightarrow p$	Time	$K^- \rightarrow \pi^+$ $K^- \rightarrow K^+$ $K^- \rightarrow p$ $\bar{p} \rightarrow \pi^+$ $\bar{p} \rightarrow p$
0.3 1.0	100 7 160 120 25	1.0	100 40 100 150 15	0.3 2.0	200 40 20 20 20	2.0	200 50 30 120 18	0.4 2.0	200 36 20 160 8
0.4 1.0	100 20 200 190 25	1.5	100 50 130 230 20	0.5 2.0	100 25 230 230 20	2.0	100 40 30 100 6	0.5 2.0	200 36 18 180
0.5 1.0	100 25 230 230 20	2.0	100 35 220 310 15	0.6 2.0	100 30 400 700 20	2.5	100 20 185 475 15	0.6 2.0	200 28 10 100
0.7 3.0	100 70 600 1500	3.0	100 10 350 390 8	0.7 3.0	100 70 600 1500	3.0	100 10 350 390 8	0.7 2.0	200 8 80
0.8 4.0	100 100 700 3200	3.0	100 230 680	0.8 4.0	100 100 700 3200	3.0	100 230 680	0.8 3.0	150 45
0.88 6.0	100 160 700 7400	3.0	100 150 875	0.88 6.0	100 160 700 7400	3.0	100 150 875	0.88 4.0	100 17

TABLE VI  
 $\pi^0$  EVENT RATE/HR FOR  $10^7$  INCIDENT PARTICLES  
 PER PULSE AND 5 PULSES/MIN

$x$	$100 \text{ GeV}/c \quad p_T = 3.0 \text{ GeV}/c$		
	$pp \rightarrow \pi^0 X$	$\pi^+ p \rightarrow \pi^0 X$	$\pi^- p \rightarrow \pi^0 X$
0.0	5.7	16.5	27.3
0.1	5.2	15.3	24.9
0.2	4.1	11.9	19.6
0.3	2.8	8.0	13.4
0.4	1.6	4.5	7.7
0.5	0.72	2.1	3.4
0.6	0.25	0.72	1.2
0.7	0.05	0.15	0.24
0.8	0.01	0.02	0.05

TABLE VII  
 ESTIMATED YIELDS FOR SELECTED CHANNELS FOR 6 HRS  
 RUNNING AT  $p_T = 0.75 \text{ GeV}/c$  and  $x = 0.3$

	<u>Evts/6 hrs</u>		<u>Evts/6 hrs</u>
$K^+ \rightarrow \pi^+$	100	$K^+ \rightarrow \pi^-$	90
$K^+ \rightarrow K^+$	120	$K^+ \rightarrow K^-$	90
$K^+ \rightarrow p$	35	$K^+ \rightarrow \bar{p}$	15
$p \rightarrow K^+$	150	$p \rightarrow \bar{K}^-$	146
		$p \rightarrow \bar{p}$	50

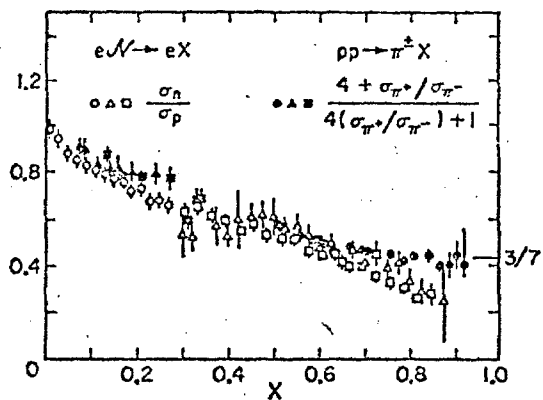


Fig. 1

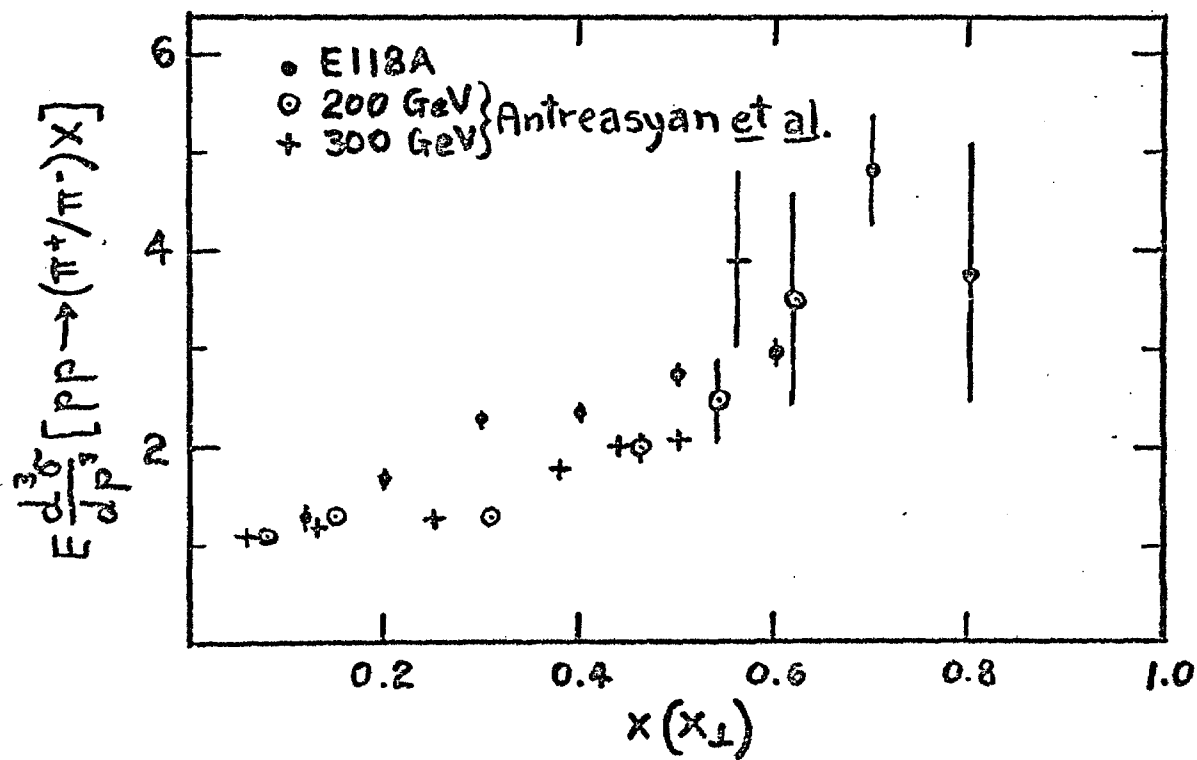


Fig. 2

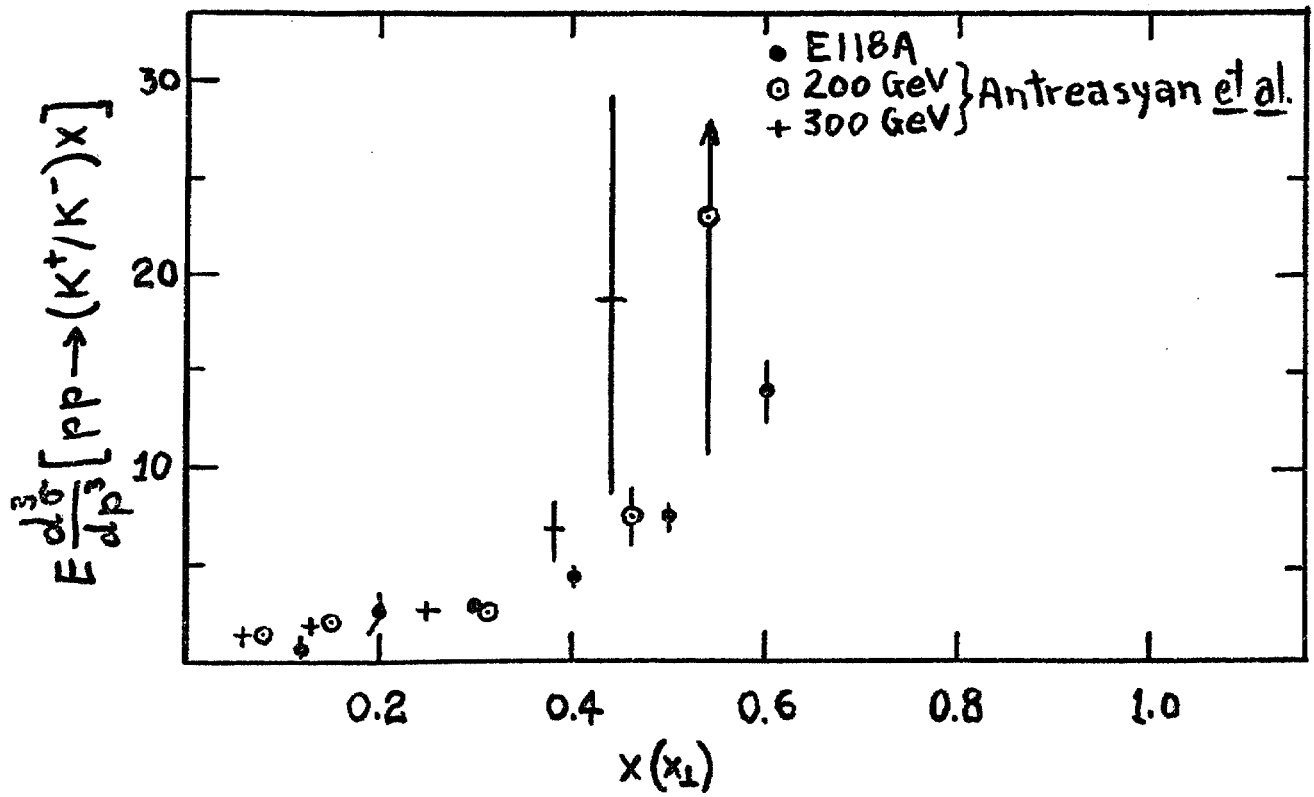


Fig. 3

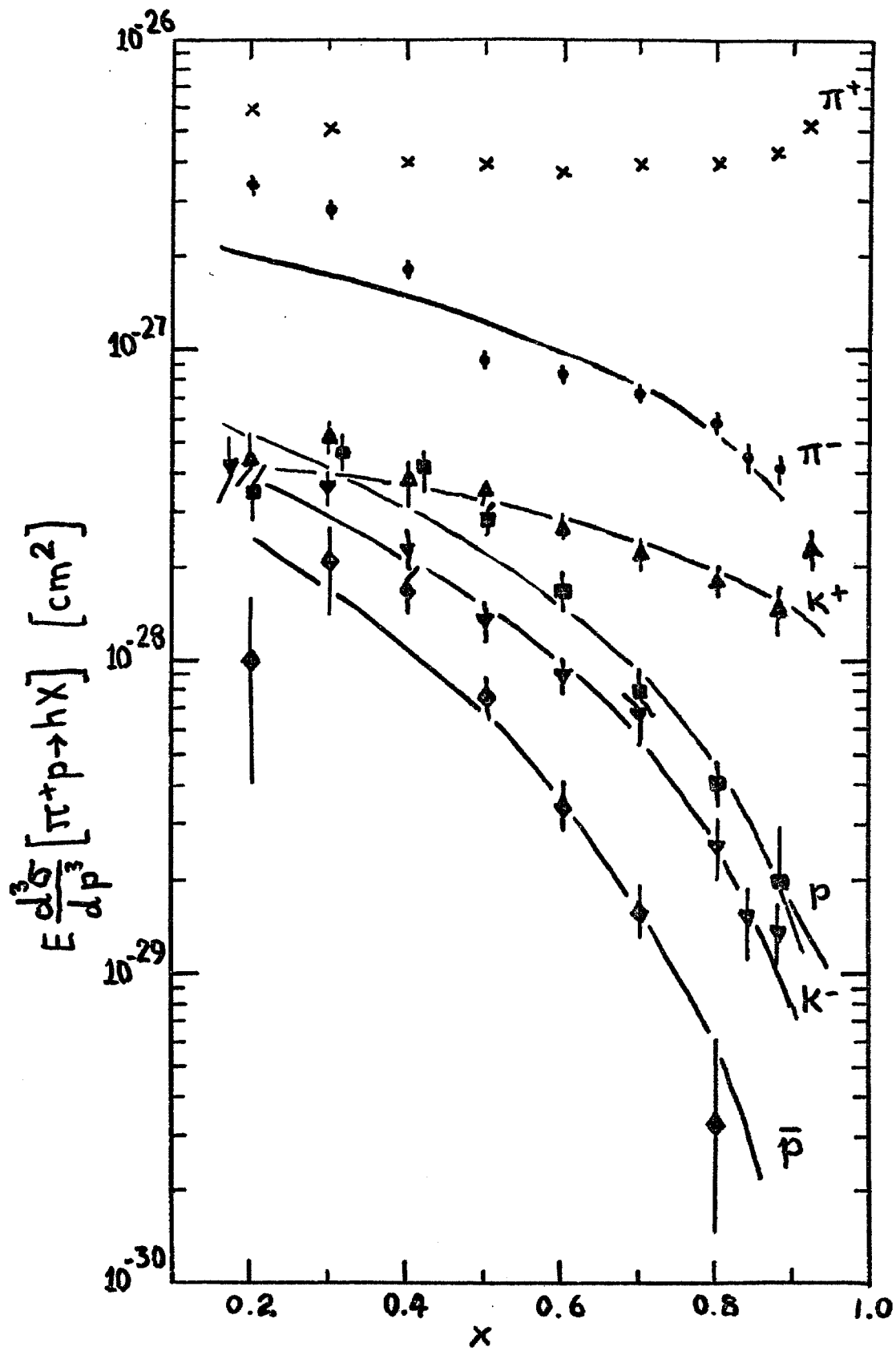


Fig. 4

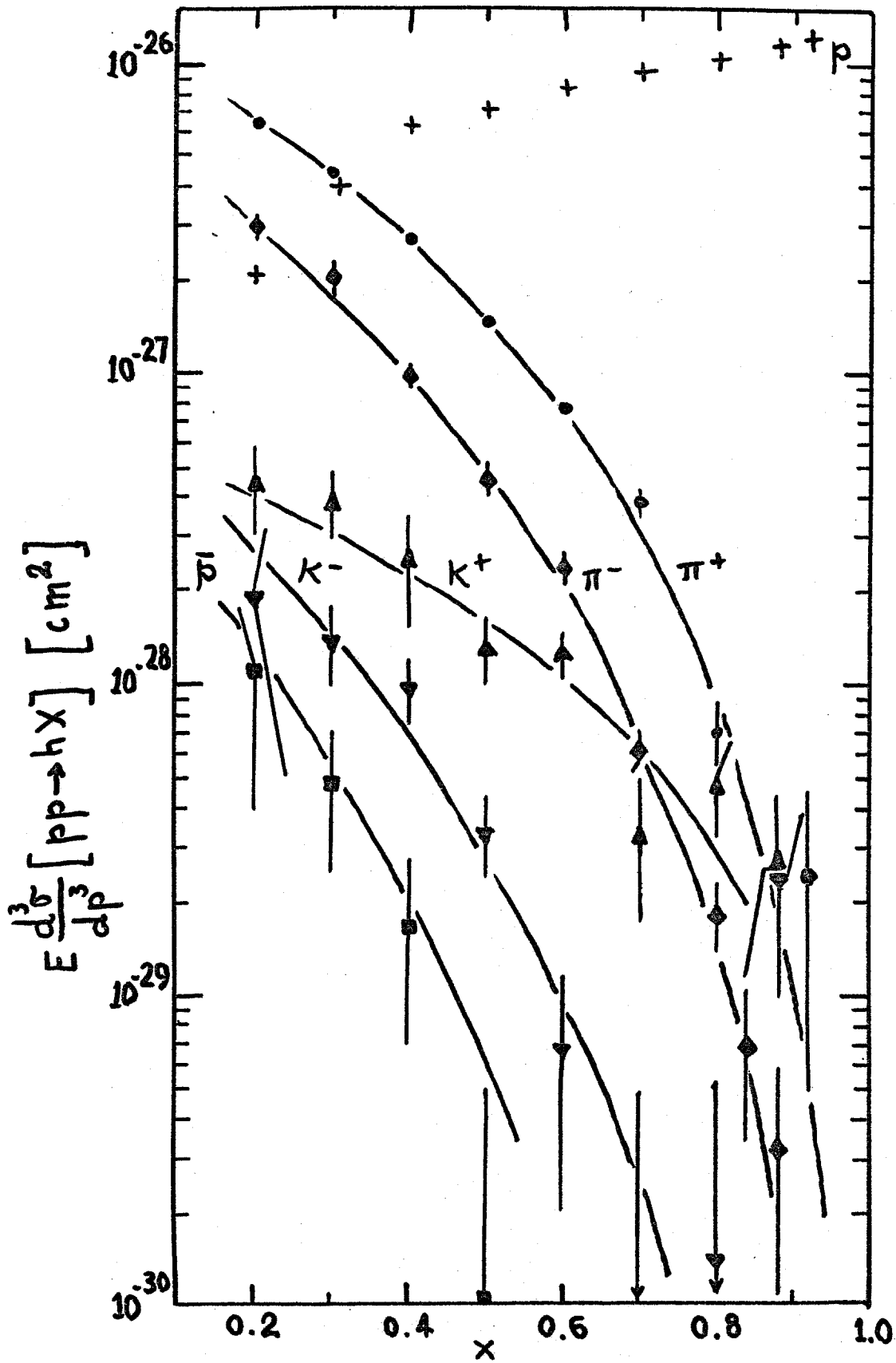
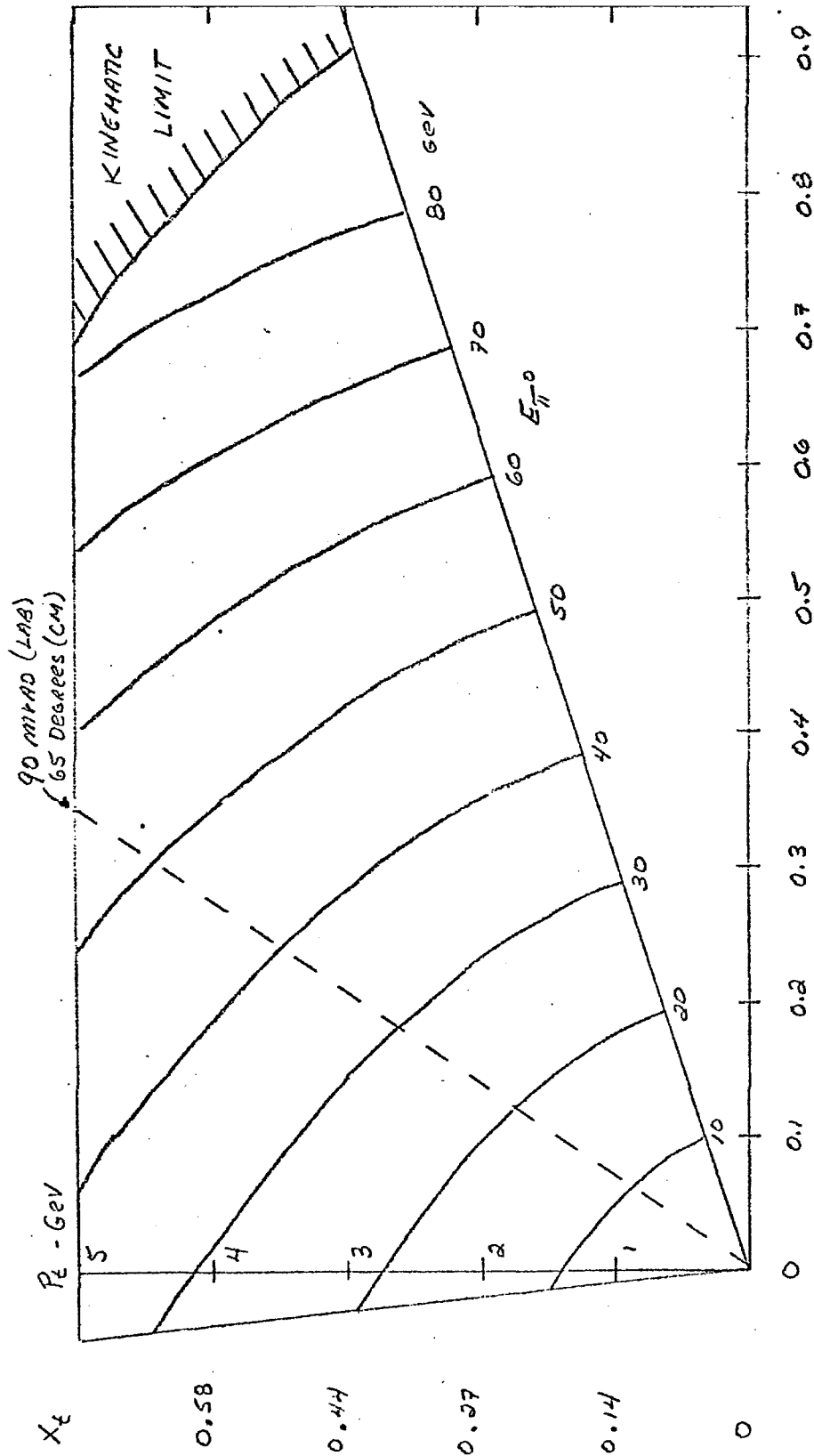


Fig. 5



$$X_L = X_{\text{FERMIAN}}$$

FIGURE 6 : 100 GEV  $\pi^0$  PRODUCTION KINEMATIC RANGE ACCEPTED BY LEAD GLASS DETECTOR